Increasing the Efficiency of the Production of 1,3,5,7-Tetranitro-1,3,5,7- tetrazocane (HMX)

Azadeh Afzali*, Karim Esmaeilpour, Sajad Damiri, Zoleikha Hadi, Mohammad Hossein Keshavarz*

Department of Chemistry, Malek-ashtar University of Technology,
Shahin-shahr P.O. Box 83145/115, Islamic Republic of Iran
*To whom correspondence should be addressed: 1) Prof. M. H. Keshavarz, Tel: (0098) 0314 522 5071;
e-mail: mhkeshavarz@mut-es.ac.ir; keshavarz7@gmail.com; or 2) A. Afzali, *e-mail:* afzali.azin@yahoo.com

Table S1. Surfaces of the independent variables of the test

Parameters	Intervals and surfaces				
	+2	+1	0	-1	-2
The quantity of 47% ammonium nitrate in nitric acid present in the reactor [mL], (X_1)	10	9.25	8.50	7.75	7
Temperature [^oC], (X_2)	53	50.50	48	45.50	43
Quantity of acetic anhydride [mL], (X_3)	15	13.75	12.50	11.25	10
Addition time of acetic anhydrite [min], (X_4)	20	17.50	15	12.50	10

Table S2. CCD design of the factors affective in HMX synthesis

No.	(X_1)	(X_2)	(X_3)	(X_4)
1	9.25	50.50	11.25	17.50
2	7.75	50.50	13.75	12.50
3	9.25	45.50	11.25	12.50
4	7.75	50.50	11.25	12.50
5	7.75	45.50	13.75	12.50
6	7.75	50.50	13.75	17.50
7	9.25	50.50	13.75	12.50
8	9.25	50.50	11.25	12.50
9	8.50	48.00	12.50	15.00
10	7.75	50.50	11.25	17.50
11	8.50	48.00	15.00	15.00
12	8.50	48.00	12.50	15.00
13	8.50	48.00	12.50	15.00
14	8.50	48.00	12.50	15.00
15	9.25	50.50	13.75	17.50
16	8.50	48.00	12.50	15.00
17	8.50	48.00	12.50	10.00
18	8.50	48.00	10.00	15.00
19	9.25	45.50	11.25	17.50
20	8.50	48.00	12.50	20.00
21	8.50	48.00	12.50	15.00
22	8.50	53.00	12.50	15.00
23	10.00	48.00	12.50	15.00
24	7.75	45.50	13.75	17.50
25	8.50	43.00	12.50	15.00
26	8.50	48.00	12.50	15.00
27	7.00	48.00	12.50	15.00
28	9.25	45.50	13.75	17.50
29	9.25	45.50	13.75	12.50
30	7.75	45.50	11.25	7.75
31	7.75	45.50	11.25	12.50

Table S3. Results of the tests and response determination

No.	Product weight [g]	Production capacity [%]	Efficiency [%]
1	9.58	14.40	54.03
2	10.32	15.28	58.20
3	10.23	15.38	57.69
4	9.75	15.00	54.99
5	10.88	16.11	61.36
6	11.66	17.27	65.76
7	10.30	14.92	58.09
8	10.26	15.42	57.86
9	10.34	15.43	58.31
10	11.29	17.36	63.67
11	10.34	14.87	58.31
12	11.31	16.88	63.81
13	9.57	14.28	53.97
14	10.19	15.21	57.48
15	10.40	15.07	58.65
16	10.71	15.99	60.45
17	11.02	16.44	62.15
18	8.93	13.84	50.36
19	8.65	13.00	48.78
20	10.96	16.35	61.81
21	10.28	15.34	57.98
22	10.20	15.22	57.52
23	11.15	16.24	62.88
24	9.65	14.29	54.42
25	7.13	10.64	40.21
26	10.17	15.17	57.36
27	6.17	9.41	34.79
28	8.90	12.89	50.19
29	9.78	14.17	55.16
30	9.48	14.58	53.46
31	9.40	14.46	53.01

Table S4. Results obtained from CCD design for the initial model

Parameter	Parameter coefficient	P value
Constant	302.385	0.007
X_1	38.556	0.338
X_2	6.957	0.304
X_3	8.798	0.001
X_4	16.076	0.824
X_1^2	1.874	0.967
X_2^2	0.081	0.106
X_3^2	0.081	0.000
X_4^2	0.323	0.060
X_1X_2	0.362	0.005
X_1X_3	0.362	0.235
X_1X_4	0.724	0.927
X_2X_3	0.109	0.050
X_2X_4	0.217	0.382
X_3X_4	0.217	0.296

Table S5. Results of the CCD design for the determination of the main model

Parameter	Parameter coefficient	P value
Constant	224.682	0.002
X_1	6.091	0.021
X_3	8.421	0.001
X_4	0.477	0.013
X_3^2	0.085	0.000
X_1X_2	0.395	0.010
X_2X_3	0.118	0.035
X_1	224.682	0.002

Table S6. Results of the CCD design for the initial model

Parameter	Parameter coefficient	P value
Constant	66.4156	0.007
X_1	8.3249	0.361
X_2	1.5012	0.163
X_3	1.9211	0.001
X_4	3.4773	0.992
X_1^2	0.4051	0.725
X_2^2	0.0177	0.022
X_3^2	0.0177	0.000
X_4^2	0.0707	0.069
X_1X_2	0.0780	0.001
X_1X_3	0.0780	0.138
X_1X_4	0.1560	0.974
X_2X_3	0.0234	0.021
X_2X_4	0.0468	0.291
X_3X_4	0.0468	0.230

Table S7. Results of the CCD design for the determination of the main model

Parameter	Parameter coefficient	P value
Constant	47.5274	0.003
X_1	1.2417	0.006
X_2	1.5097	0.020
X_3	1.7608	0.001
X_4	0.0972	0.013
X_2^2	0.0179	0.006
X_3^2	0.1790	0.000
X_1X_2	0.0805	0.002
X_2X_3	0.0242	0.009

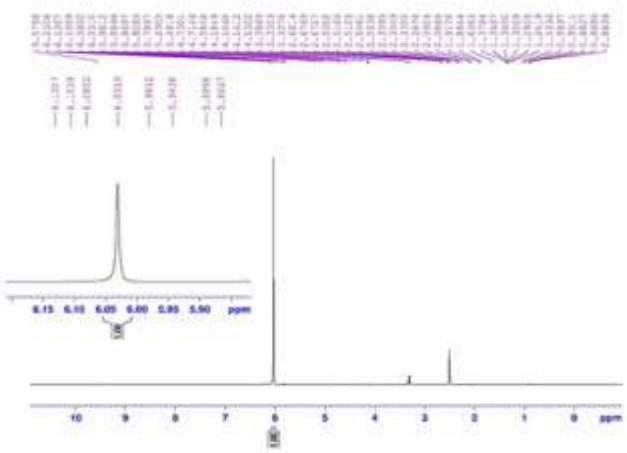

Figure S1. ^{1}H NMR spectrum, HMX product.

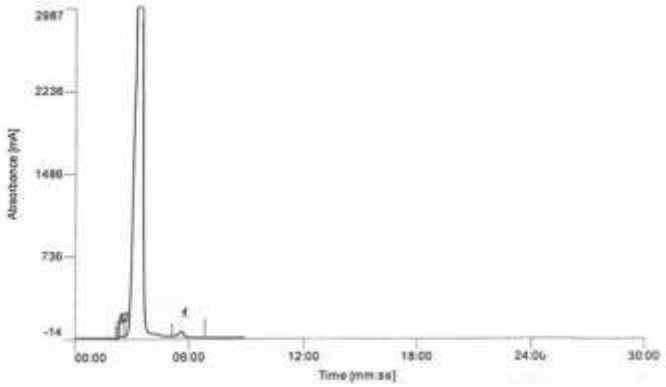

Figure S2. Chromatograph of pure HMX.

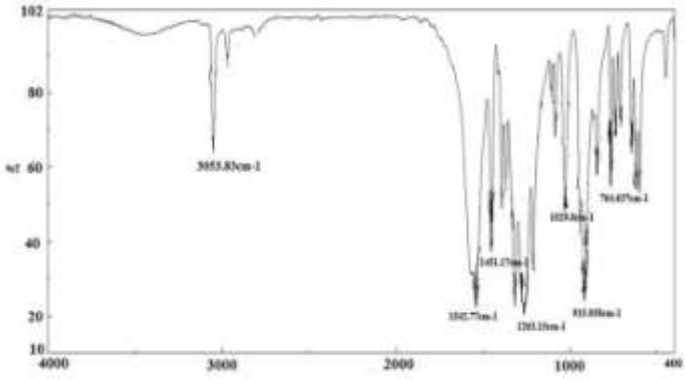

Figure S3. FT-IR spectrum for β-HMX product.

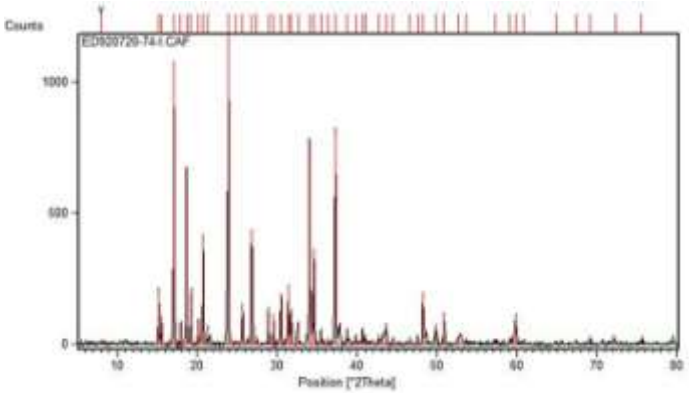

Figure S4. XRD overlapped pattern of the sample.

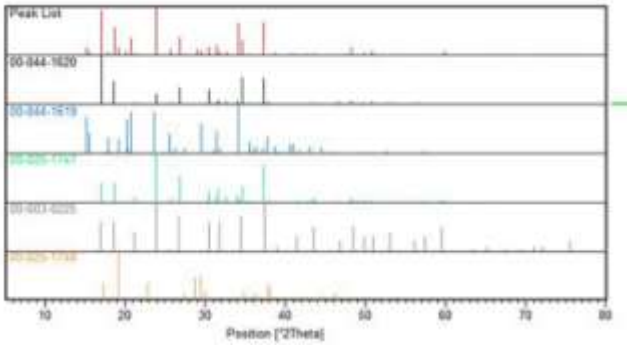

Figure S5. Separate XRD patterns of the sample.

Figure S6. Microscopic image of the sample at a magnification of 100X.

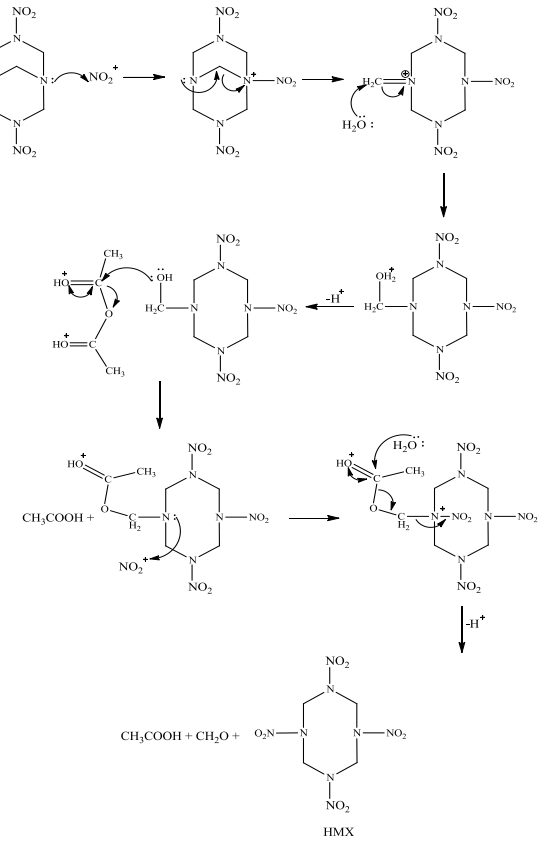

Figure S7. The suggested mechanism for the conversion of DPT to HMX.

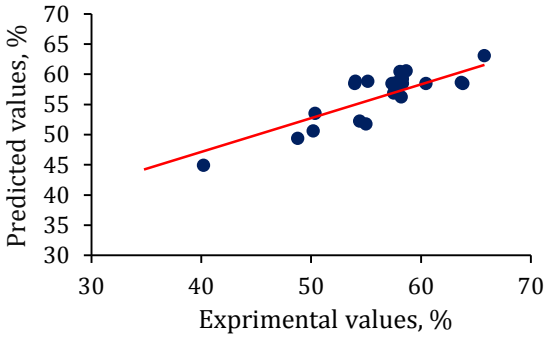

Figure S8. Linear correlation of experimental values against the predicted values of Eqs. (4) and (5).

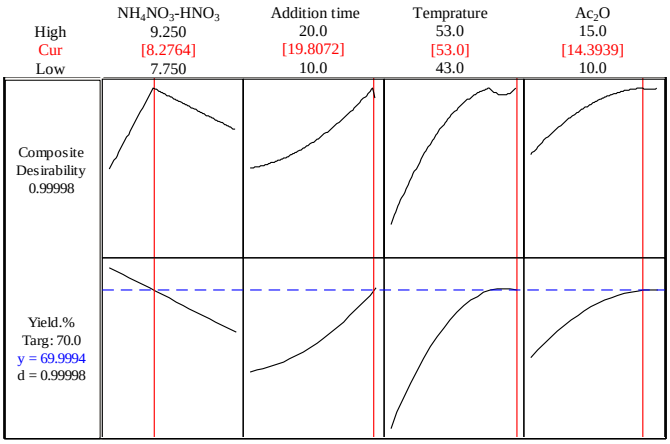

Figure S9. The optimized diagram of the parameters influencing the HMX efficiency.

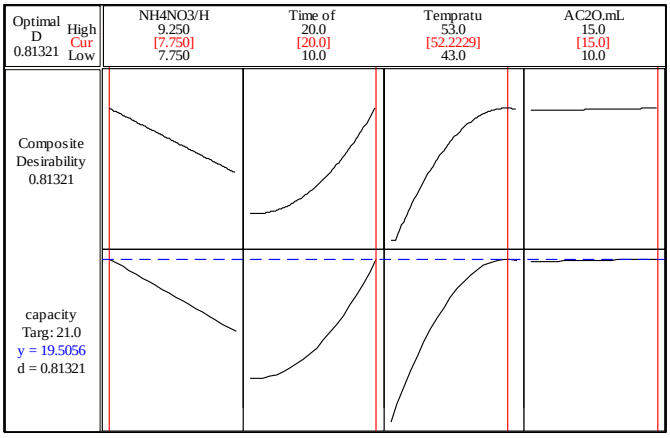

Figure S10. The optimized diagram of the effective parameters in the capacity of HMX production.

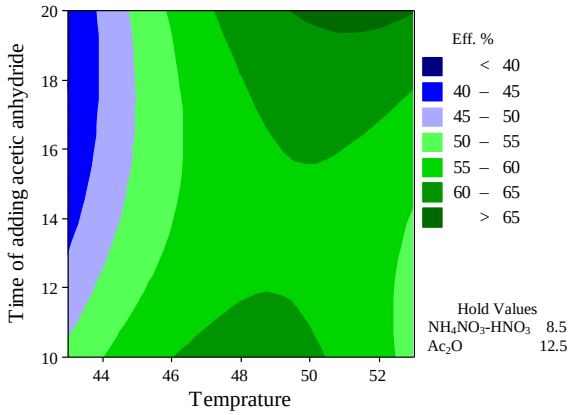

Figure S11. Contour plot for efficiency as a function of temperature.

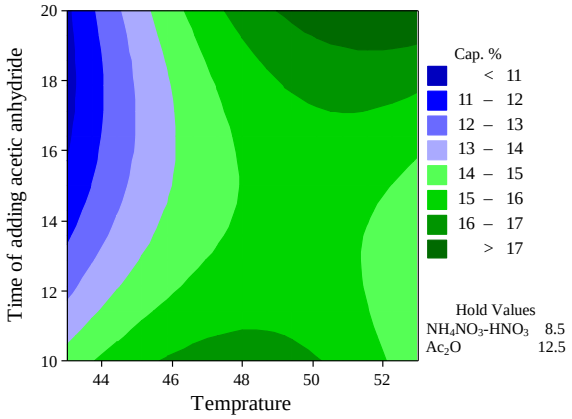

Figure S12. Contour plot for production capacity as a function of temperature.

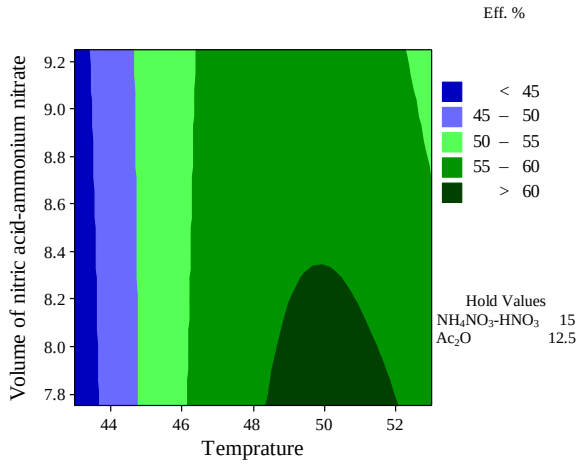

Figure S13. Contour plot for efficiency as a function of temperature and volume of ammonium nitrate/nitric acid solution.

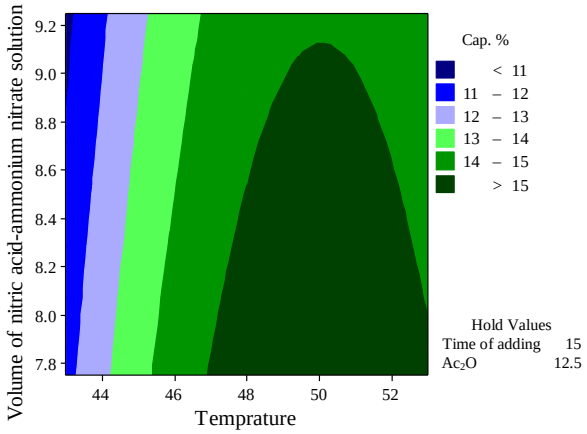

Figure S14. Contour plot for production capacity as a function of temperature and volume of ammonium nitrate/nitric acid solution.

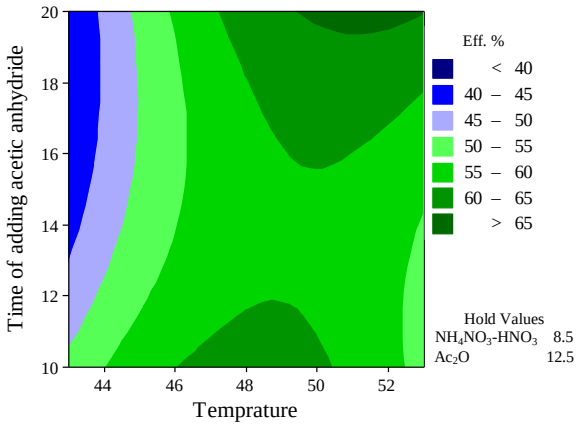

Figure S15. Efficiency contour plot as a function of temperature and loss time of acetic anhydride.

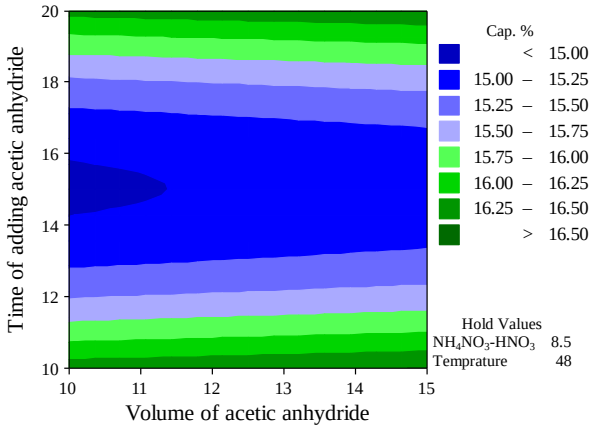

Figure S16. Production capacity contour plot as a function of acetic anhydrite volume and addition time of acetic anhydride.

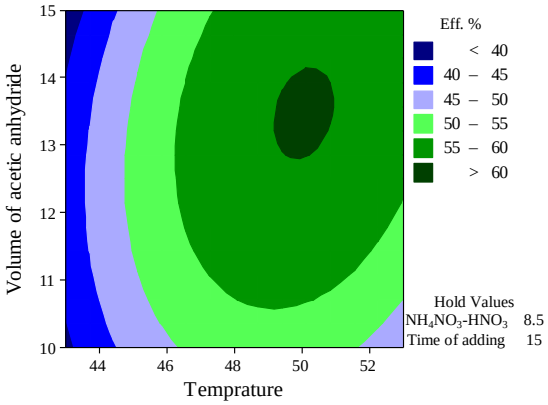

Figure S17. Contour plot for efficiency as a function of temperature and volume of acetic anhydride.

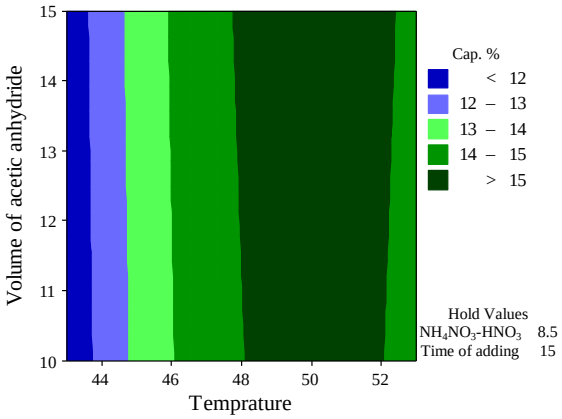

Figure S18. Contour plot for production capacity as a function of temperature and volume of acetic anhydride.